AGU PUBLICATIONS

Geophysical Research Letters

RESEARCH LETTER
10.1002/2014GL060097

Key Points:
- The 2013 Rueisuei earthquake illuminates enigmatic Central Range fault
- Finite-fault slip inversion shows the fault is west dipping and reverse
- The fault may bound a doubly vergent Taiwan orogenic wedge

Supporting Information:
- Text S1
- Figure S1
- Figure S2

Correspondence to:
R. Y. Chuang,
chuangyu@indiana.edu

Citation:
Chuang, R. Y., K. M. Johnson, Y.-T. Kuo, Y.-M. Wu, C.-H. Chang, and L.-C. Kuo (2014), Active back thrust in the eastern Taiwan suture revealed by the 2013 Rueisuei earthquake: Evidence for a doubly vergent orogenic wedge?, *Geophys. Res. Lett.*, *41*, 3464–3470, doi:10.1002/2014GL060097.

Received 1 APR 2014
Accepted 9 MAY 2014
Accepted article online 13 MAY 2014
Published online 28 MAY 2014

Active back thrust in the eastern Taiwan suture revealed by the 2013 Rueisuei earthquake: Evidence for a doubly vergent orogenic wedge?

Ray Y. Chuang[1], Kaj M. Johnson[1], Yu-Ting Kuo[2], Yih-Min Wu[2], Chien-Hsin Chang[3], and Long-Chen Kuo[4]

[1]Department of Geological Sciences, Indiana University, Bloomington, Bloomington, Indiana, USA, [2]Department of Geosciences, National Taiwan University, Taipei, Taiwan, [3]Central Weather Bureau, Taipei, Taiwan, [4]Institute of Earth Sciences, Academia Sinica, Taipei, Taiwan

Abstract Rapid exhumation of 3–10 mm/yr of the Taiwan metamorphic range is often explained as the unroofing of the retrowedge of a doubly vergent mountain belt. Yet, to date, the Central Range fault forming the boundary of the retrowedge has displayed no definitive evidence for recent seismic activity and no unambiguous geomorphic expression over much of the fault. The 2013 *M*6.4 Rueisuei reverse-faulting earthquake nucleated at the eastern boundary of the retrowedge and appears to illuminate the west dipping Central Range fault. We estimate the fault geometry and coseismic slip distribution using a uniform stress drop slip inversion and surface displacements derived from GPS and strong-motion data. We identify a ~42° dipping blind reverse fault, consistent with the previously proposed buried Central Range fault beneath the highly active Longitudinal Valley fault. This earthquake may be the first indication that rapid exhumation and uplift occur along a distinct fault structure bounding the eastern margin of the Taiwan retrowedge.

1. Introduction

The Taiwan mountain belt, which is deforming by collision between the Luzon arc and Chinese continental margin, (Figure 1) [e.g., *Suppe*, 1981; *Byrne et al.*, 2011] has been analyzed with the theory of critical taper wedge mechanics [*Suppe*, 1981; *Davis et al.*, 1983; *Dahlen et al.*, 1984; *Barr and Dahlen*, 1989; *Barr et al.*, 1991; *Suppe*, 2007] and interpreted as an orogenic wedge developing above a detachment at or above the top of the east dipping Eurasian slab [*Suppe*, 1981; *Davis et al.*, 1983; *Carena et al.*, 2002; *Yue et al.*, 2005]. However, since critical taper mechanics views the orogen as a singly vergent wedge and does not explicitly consider the role of structures at the retrowedge, the model is not able to explain 3–10 mm/yr unusually high rates of exhumation and uplift [*Liu et al.*, 2001; *Dadson et al.*, 2003; *Willett et al.*, 2003; *Beyssac et al.*, 2007; *Kirstein et al.*, 2010; *Ching et al.*, 2011a] at the eastern wedge. On the other hand, models with doubly vergent wedges and a retroshear structure [*Willett et al.*, 1993; *Willett and Brandon*, 2002; *Fuller et al.*, 2006] may be able to explain the rapid rates. The boundary at the retrowedge between the Central Range to the west and the Longitudinal Valley to the east was long ago named the Central Range fault [*Biq*, 1965]. This fault is also considered to be one of the major faults, in addition to the Longitudinal Valley fault, of the Longitudinal Valley suture that marks the ongoing collision of the Luzon volcanic arc with the Eurasian margin [e.g., *Shyu et al.*, 2006]. However, to date there has been no definitive evidence of recent seismic activity on the Central Range fault north of the 2006 Taitung earthquake (Figure 1). There is also no unambiguous geomorphic expression of the northern portion of the Central Range fault north of Rueisuei [*Willemin and Knuepfer*, 1994; *Shyu et al.*, 2006] where deformation in the suture zone is complicated by northwestward motion of the Philippine Sea plate under Taiwan [e.g., *Lallemand et al.*, 2013]. Therefore, it remains unclear what role the Central Range fault plays in mountain building and whether the fault even exists as a distinct structure in eastern Taiwan.

The paucity of geological and geophysical evidence has led to discordant views on the existence and type of motion on the Central Range fault in numerous studies over the years. This boundary has been interpreted variably as a contact between metamorphic rocks and overlying sediments [e.g., *Chang et al.*, 2000; *Malavieille et al.*, 2002; *Malavieille and Trullenque*, 2009], an east dipping normal fault [e.g., *Crespi et al.*, 1996; *Lee et al.*, 2001, 2003; *Bertrand et al.*, 2012], an east dipping strike-slip fault [e.g., *Huang et al.*, 2006] and a west dipping reverse fault [e.g., *Teng and Lin*, 2004; *Shyu et al.*, 2005, 2006]. Detailed field mapping of the Central Range

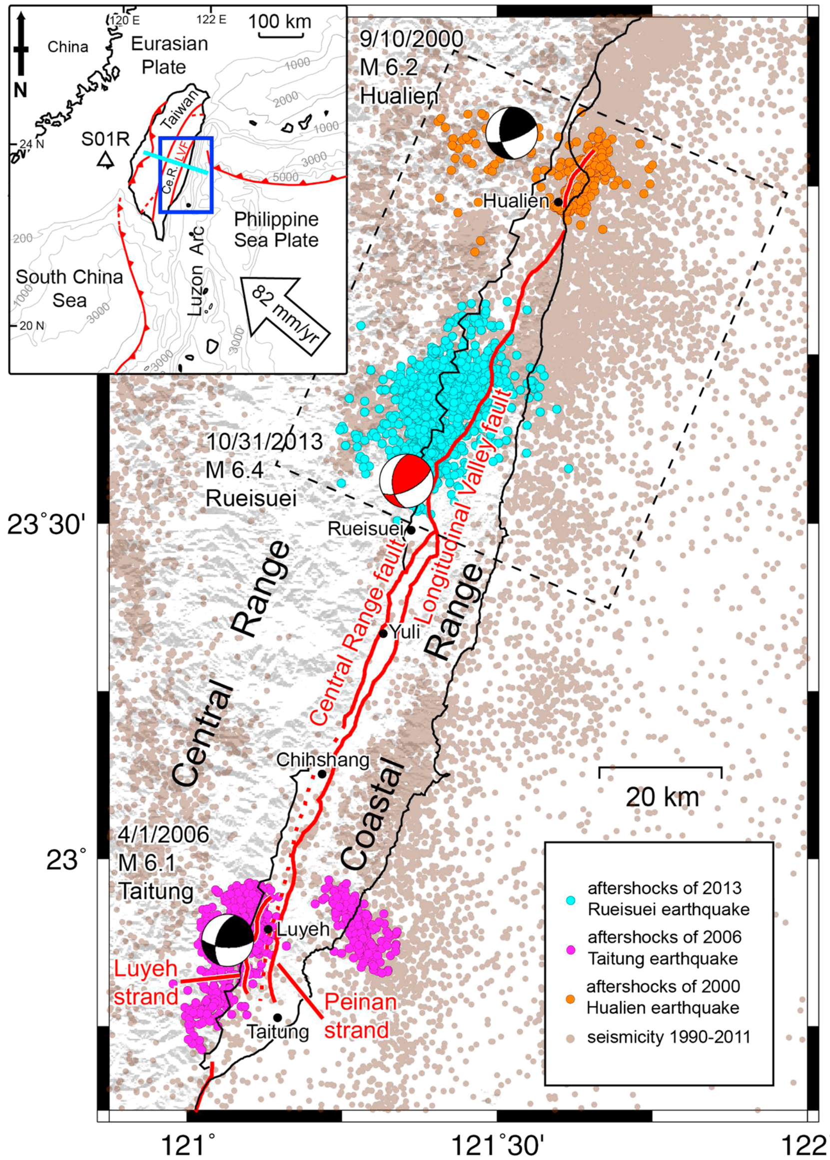

Figure 1. Active faults and seismicity around the Longitudinal Valley, eastern Taiwan. Red lines are fault traces based on *Shyu et al.* [2005], and dashed red line is inferred location of buried Central Range fault. Irregular black line denotes mountain front of Central Range. Beach balls are 2000 Hualien (black), 2006 Taitung (black), and 2013 Rueisuei (red) main shocks. Grey dots are $M > 3$ relocated seismicity from 1990 to 2011. Cyan, magenta, and orange dots are aftershocks of the 2013 Rueisuei, 2006 Taitung, and 2000 Hualien earthquakes, respectively. Seismicity within dashed-line box is plotted in Figure 3. Inset shows tectonic setting of Taiwan. Cyan line is cross section of Figure 4. S01R (Paisha station) is the reference GPS site. White arrow denotes plate convergence rate from *Yu et al.* [1997]. LVF: Longitudinal Valley fault; Ce.R.: Central Range.

fault by *Shyu et al.* [2006] identified the fault trace from geomorphic features in the central Longitudinal Valley between Rueisuei and Chihshang (Figure 1). Studies of ambient seismicity and repeating earthquakes [*Kuochen et al.*, 2004; *Rau et al.*, 2007; *Chen et al.*, 2009b] infer a west dipping fault in the northern Longitudinal Valley, but they interpret the structure to be the Longitudinal Valley fault, a major oblique fault with sinistral reverse motion in the eastern valley. In the southernmost valley, the 2006 *M*6.1Taitung earthquake and its aftershocks delineate a high-angle fault along the eastern flank of the Central Range south of Luyeh [*Wu et al.*, 2006; *Chen et al.*, 2009a; *Mozziconacci et al.*, 2013] (Figure 1), which is interpreted to be associated with the Central Range fault [*Wu et al.*, 2006; *Mozziconacci et al.*, 2013] even though the focal mechanism solution is mainly strike slip. The treatment of the Central Range fault in numerical studies is also varied. Some models ignore the fault [e.g., *Willett et al.*, 2001; *Hsu et al.*, 2003; *Mouyen et al.*, 2009], whereas at least one model

10.1002/2014GL060097

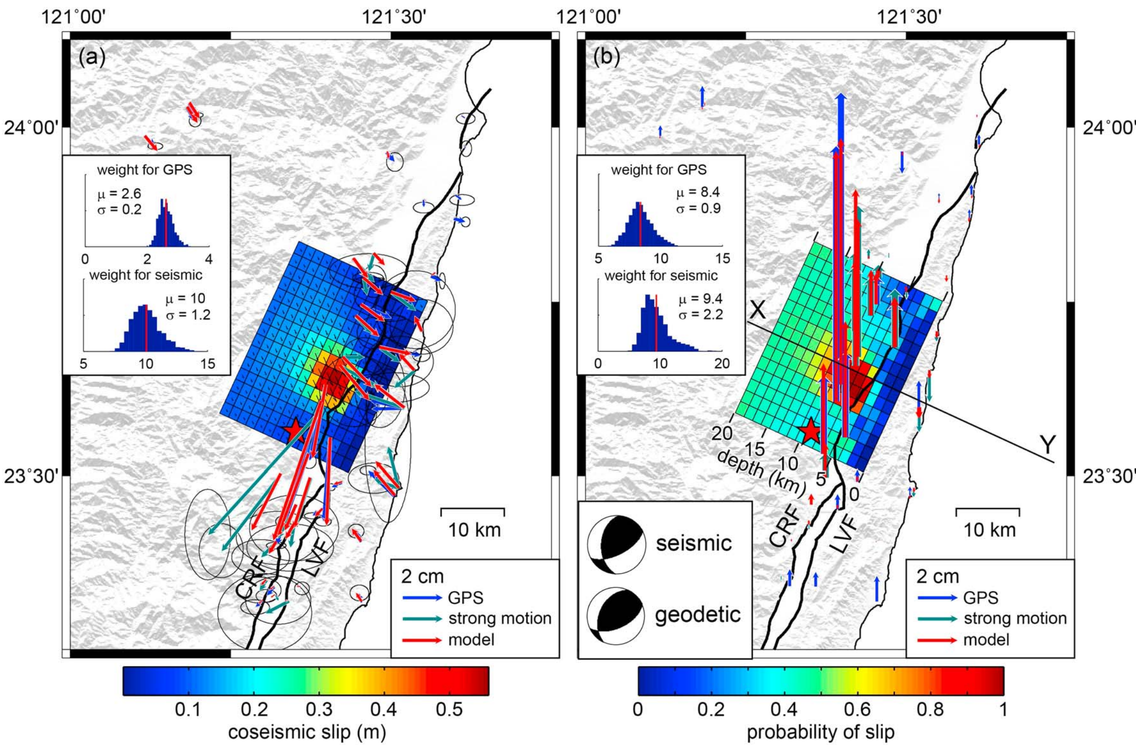

Figure 2. (a) Mean coseismic slip distribution and model fit to horizontal displacements of 2013 Rueisuei earthquake. Blue arrows are observations from GPS, blue-grey arrows are from strong motion, and red arrows are model vectors. Error ellipses show 95% confidence level. The left inset shows posterior probability distributions of relative weights of −2 uncertainties for data from GPS and strong motion. CRF: Central Range fault; LVF: Longitudinal Valley fault. (b) Probability of slip and model fit to vertical displacements of 2013 Rueisuei earthquake. Colored rectangles represent the mean of binary slip parameter where 0 means the patch did not slip and 1 indicates the patch slips coseismically. Line *XY* is location of cross section in Figure 3. Lower left inset compares seismic and geodetic focal mechanisms.

represents it as a normal fault [e.g., *Simoes et al.*, 2007]. Numerical models of present-day vertical motions show that slip on the Central Range fault improves the fit of vertical motion recorded with GPS data [*Johnson et al.*, 2005; *Huang et al.*, 2010; *Ching et al.*, 2011a].

The 2013 *M*6.4 Rueisuei earthquake is the first reverse-slip event providing seismic and geodetic constraints on fault activity (Figure 1) and uplift of the Central Range side (footwall) of the northern Longitudinal Valley fault. We conduct a joint inversion of coseismic displacements derived from GPS and strong-motion data for fault geometry and slip distribution and show that the northern Central Range fault is indeed active. We suggest that this result together with the observations from *Shyu et al.* [2006] and the 2006 Taitung earthquake indicates that the entire Central Range fault is the active structure bounding the retrowedge and contributing to mountain building in Taiwan.

2. Data and Joint Inversion

In order to characterize coseismic displacements for the Rueisuei earthquake, we use surface displacement data derived from strong-motion seismometers and continuously recording GPS. We acquired phase data from 25 strong-motion stations of the Taiwan Strong-Motion Instrumentation Program of the Central Weather Bureau (CWB) in Taiwan. We adopt the method of *Wu et al.* [2006] to integrate acceleration records twice with baseline corrections [*Wu and Wu*, 2007] (Figure S1) in order to obtain coseismic displacements (Figure 2). We use continuous GPS data from 48 stations processed by the Taiwan Earthquake Research Center (TEC) GPS lab (data source: http://gps.earth.sinica.edu.tw). The coseismic displacements (Figure 2) are determined by differencing 4 and 3 day average GPS positions before and after the main shocks, respectively, with respect to the Paisha station (S01R) (Figure 1). The maximum coseismic displacements are 43 mm and 66 mm in the horizontal and vertical directions, respectively. We relocate the main shock and aftershocks by using the 3-D location method of *Wu et al.* [2008] with 3-D tomography data based on *Wu et al.* [2009] to

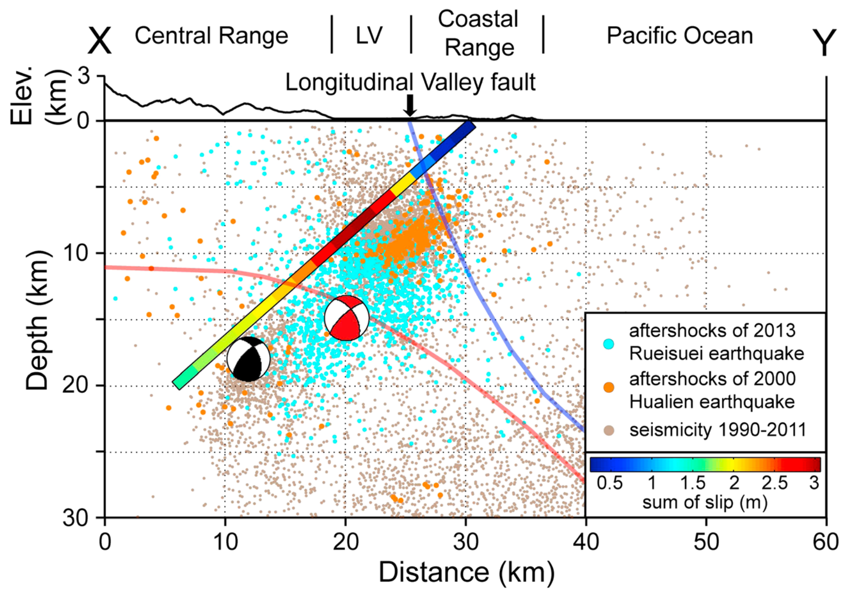

Figure 3. Cross section of model fault plane looking from southwest parallel to the strike of model fault plane. Color bar indicates model fault plane with sum of slip over patches at the same depth. Model fault plane is slightly above seismicity possibly due to simplified elastic structures and earthquake relocation errors. Most slip occurred at depths between 4 and 15 km. Red and black focal mechanism solutions show the Rueisuei and Hualien earthquake, respectively. Blue line is Longitudinal Valley fault after *Shyu et al.* [2005], and red line is Taiwan main detachment proposed by *Carena et al.* [2002]. LV: Longitudinal Valley. Seismicity symbols are same as those in Figure 1.

compare with our model results. We process seismicity for 15 days after the Rueisuei main shock to identify the aftershocks. In order to further explain the seismogenic structure in the western valley, we also relocate the main shock of the 2000 Hualien earthquake and aftershocks within 2 months of the main shocks. The azimuthal distribution of the local seismic network is not optimal since most of the stations are located west of the seismicity. It is well known that this geometry can produce a systematic bias in the location of earthquakes.

In order to characterize the fault geometry, we use a probabilistic, Bayesian inversion technique with the Markov chain Monte Carlo Metropolis algorithm to solve for slip distributions and fault orientations simultaneously. We use a homogenous elastic model with the mechanical constraint of uniform stress drop based on *Sun et al.* [2011], also adopted by *Ching et al.* [2011b] and *Chuang et al.* [2013]. In the inversion, we solve for fault parameters including position, strike, dip, and two components of stress drop with fixed fault plane size (length and width of 30 km) and depth (the top of the fault plane on the surface). The fault planes are discretized into 225 patches in total (15 in each direction). We solve for a binary slip parameter that determines whether or not the patch slipped during the earthquake. The Bayesian inversion also provides an objective basis to weigh the two different types of data sets: GPS and strong-motion-derived displacements.

3. Results

Figure 2 shows the mean estimated slip distribution, the probability that an individual patch slipped in the earthquake, and fits to the horizontal and vertical observations. The fits to the data are generally good except some fits to the horizontal strong-motion data. The other model parameters estimated in the Bayesian inversion are shown in Figure S2. Estimated strike-slip and dip-slip components of coseismic stress drop are -1.4 ± 0.2 MPa (left lateral) and 2.0 ± 0.3 MPa (reverse), respectively. The model fault is west dipping (strike of 201°–209° and dip of 39°–44°; Figure S2). The average slip of 0.13 m with maximum slip of 0.56 m is concentrated at depths between 4 and 15 km (Figure 3). The average rake is 57° (0° means left-lateral movement and 90° means reverse movement), indicating primarily reverse sense of slip with left-lateral motion. The computed moment tensor from our model result agrees well with the seismic focal mechanism solution (Figure 2b). The model fault plane is located slightly above the distributions of the aftershocks, similar to other studies [e.g., *Ching et al.*, 2011b; *Chuang et al.*, 2013]. This is likely a consequence of the assumed homogeneous elastic properties. It would require lower elastic moduli at shallow depths to fit data

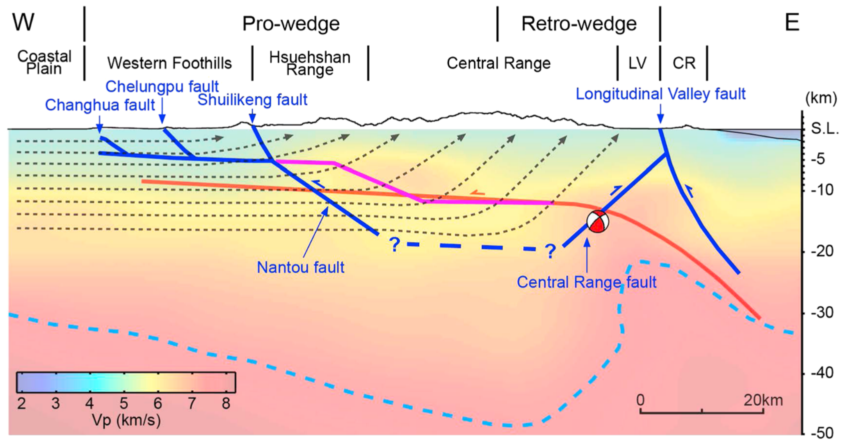

Figure 4. Cross section of Taiwan orogenic wedge. Blue lines are major faults after *Chuang et al.* [2013]. Red line is proposed Taiwan main detachment by *Carena et al.* [2002], and pink line is proposed detachment by *Yue et al.* [2005]. Dashed black lines are hypothetical material flow lines of doubly vergent wedge after *Willett and Brandon* [2002] and *Fuller et al.* [2006]. Focal mechanism shows the Rueisuei earthquake. *P* wave velocity tomography image is from *Kuo-Chen et al.* [2012]. Dashed blue line indicates isosurface of 7.5 km/s *P* wave velocity. CR: Coastal Range; LV: Longitudinal Valley.

with a deeper fault plane [e.g., *Chuang et al.*, 2013]. We estimate a seismic moment of 3.44×10^{18} N m and a moment magnitude of 6.36 assuming a shear modulus of 30 GPa, in agreement with CWB catalog of $M_w = 6.4$.

4. Discussion and Conclusions

While the east dipping, reverse-slip Longitudinal Valley fault (Figure 2) is the only recognizable fault at the surface in the northern valley, the Rueisuei earthquake uplifted the footwall side of the Longitudinal Valley fault, requiring the existence of an additional fault in the northern valley. The inferred slip on the west dipping fault is consistent with the geometry of the thrusting Central Range fault proposed in other studies [e.g., *Yen*, 1965; *Shyu et al.*, 2006]. At the southern end of the Longitudinal Valley, the model results of the 2006 Taitung earthquake also show similar but steeper fault geometry [*Wu et al.*, 2006; *Chen et al.*, 2009a; *Mozziconacci et al.*, 2013]. The lateral extension of the model Rueisuei fault and the distribution of aftershocks correlates well with the surface mapping of the Central Range fault around Rueisuei [*Shyu et al.*, 2006] (Figure 2), and the lack of coseismic slip above 4 km depth is also consistent with the interpretation that the Central Range fault is buried beneath the Longitudinal Valley fault [*Shyu et al.*, 2005, 2006] (Figure 3). The Rueisuei earthquake demonstrates that the Central Range fault is clearly active north of Rueisuei contradicting the interpretation by *Shyu et al.* [2006] that the fault is inactive. Note that the correlation between the Rueisuei fault plane, ambient seismicity, and the main shock and aftershocks of the 2000 Hualien earthquake suggests that the northward trend of the Central Range fault seems to maintain the same fault geometry (Figure 3). We suggest that the 2000 Hualien earthquake, which had not yet been well studied before, also occurred on the Central Range fault. Although the Rueisuei earthquake was concentrated at depths of 4—15 km, aftershocks and background seismicity are deeper, showing that the fault is active to at least 20 km depth, which is deeper than the thin-skinned detachment proposed by *Carena et al.* [2002] (Figure 3).

Our result together with the observation from *Shyu et al.* [2006] and the 2006 Taitung earthquake illuminates the geometry of the reverse Central Range fault along the entire length Longitudinal Valley, consistent with the retrothrusting structure of the doubly vergent orogenic wedge [*Silver and Reed*, 1988; *Willett et al.*, 1993; *Willett and Brandon*, 2002; *Fuller et al.*, 2006; *Fisher et al.*, 2007] (Figure 4) and consistent with the numerical models incorporating a reverse fault to fit present-day vertical geodetic data of the orogen [*Johnson et al.*, 2005; *Ching et al.*, 2011a]. Although critical taper mechanics can be used to estimate the geometry of the back thrust, it predicts a gently dipping retrowedge detachment of ~5° similar to the prowedge detachment geometry [e.g., *Suppe*, 1981], which is significantly less than ~42° dip inferred from this study. Laboratory studies and kinematic models show that the geometry of the back thrust influences the geometry and deformation of the retrowedge [e.g., *Rossetti et al.*, 2002; *Simoes et al.*, 2007]. Laboratory experiments show that the geometry of the retrowedge back thrust may also reflect the strength of the basal detachment [*Malavieille and Trullenque*, 2009]. The inferred fault geometry from this study may be used to constrain the wedge deformation.

The reverse fault geometry may suggest that the Central Range fault is contributing to the uplift of the orogen as reflected by our modeling of the coseismic displacements. However, one could associate the west dipping fault in northern valley with the westward motion of the Philippine Sea plate beneath the Central Range [e.g., *Wu et al.*, 2009] or the incipient northwestward underthrusting of the Philippine Sea plate [e.g., *Lallemand et al.*, 2013]. In the latter case, slip on the fault that ruptured in the Rueisuei earthquake would not necessarily contribute to long-term uplift of the Central Range, and therefore, the fault would be part of the back thrust of the doubly vergent wedge in terms of geometry rather than dynamics. Without observations of the interseismic vertical deformation across this region [e.g., *Ching et al.*, 2011a], it is not possible to know for sure that mountain building is being accommodated along this fault. However, previous studies suggest the underthrusting associated with subduction occurs farther offshore [e.g., *Malavieille et al.*, 2002; *Lallemand et al.*, 2013], so if this is indeed an underthrusting event, the Rueisuei earthquake requires a modification of the underthrusting model to incuse onshore faulting.

Although a thin-skinned model [*Carena et al.*, 2002; *Yue et al.*, 2005] previously proposed a widespread shallow detachment under much of Taiwan (Figure 4), the recent 2013 Nantou earthquake series and the Rueisuei earthquake suggest that faulting extends deeper than this shallow detachment. The 2013 Nantou earthquakes illuminate the Nantou ramp fault extending to ~20 km depth under the Taiwan fore wedge [*Chuang et al.*, 2013] (Figure 4). Similarly, the Central Range fault appears to extend to at least a depth of 20 km under the retrowedge. It is possible that these newly identified active faults bound a doubly vergent orogenic wedge that extends deeper than the proposed shallow detachment (Figure 4).

Acknowledgments
We thank the Central Weather Bureau, Taiwan, for providing seismic data. We thank the GPS lab of the Taiwan Earthquake Research Center (TEC) at the Institute of Earth Sciences, Academia Sinica, Taiwan (http://gps.earth.sinica.edu.tw), for providing coseismic GPS displacement data. We thank two reviewers, Michael Hamburger, J. Bruce H. Shyu, Hsin-Hua Huang, and Te-Cheng Yi for their helpful suggestions. This research was supported by the TEC funded through Ministry of Science and Technology (MOST). The TEC contribution number for this article is 00101.

The Editor thanks Jonathan Lewis and an anonymous reviewer for their assistance in evaluating this paper.

References

Barr, T. D., and F. A. Dahlen (1989), Brittle frictional mountain building: 1. Deformation and mechanical energy budget, *J. Geophys. Res.*, *94*, 3906–3922, doi:10.1029/JB094iB04p03906.

Barr, T. D., F. A. Dahlen, and D. C. McPhail (1991), Brittle frictional mountain building: 3. Low-grade metamorphism, *J. Geophys. Res.*, *96*, 10,319–10,338, doi:10.1029/91JB00295.

Bertrand, E. A., M. J. Unsworth, C. W. Chiang, C. S. Chen, C. C. Chen, F. T. Wu, E. Türkoğlu, H. L. Hsu, and G. J. Hill (2012), Magnetotelluric imaging beneath the Taiwan orogen: An arc-continent collision, *J. Geophys. Res.*, *117*, B01402, doi:10.1029/2011JB008688.

Beyssac, O., M. Simoes, J. P. Avouac, K. A. Farley, Y. G. Chen, Y. C. Chan, and B. Goffé (2007), Late Cenozoic metamorphic evolution and exhumation of Taiwan, *Tectonics*, *26*, TC6001, doi:10.1029/2006TC002064.

Biq, C. (1965), The eastern Taiwan rift, *Petrol. Geol. Taiwan*, *4*, 93–106.

Byrne, T., Y. C. Chan, R. J. Rau, C. Y. Lu, Y. H. Lee, and Y. J. Wang (2011), The arc-continent collision in Taiwan, in *Arc-Continent Collision*, edited by D. Brown and P. D. Ryan, pp. 213–246, Springer, New York.

Carena, S., J. Suppe, and H. Kao (2002), Active detachment of Taiwan illuminated by small earthquakes and its control of first-order topography, *Geology*, *30*, 935–938.

Chang, C. P., J. Angelier, and C. Y. Huang (2000), Origin and evolution of a mélange: The active plate boundary and suture zone of the Longitudinal Valley, Taiwan, *Tectonophysics*, *325*, 43–62.

Chen, H. Y., Y. J. Hsu, J. C. Lee, S. B. Yu, L. C. Kuo, Y. L. Jiang, C. C. Liu, and C. S. Tsai (2009a), Coseismic displacements and slip distribution from GPS and leveling observations for the 2006 Peinan earthquake (Mw 6.1) in southeastern Taiwan, *Earth Planets Space*, *61*, 299–318.

Chen, K. H., R. J. Rau, and J. C. Hu (2009b), Variability of repeating earthquake behavior along the Longitudinal Valley fault zone of eastern Taiwan, *J. Geophys. Res.*, *114*, B05306, doi:10.1029/2007JB005518.

Ching, K. E., M. L. Hsieh, K. M. Johnson, K. H. Chen, R. J. Rau, and M. Yang (2011a), Modern vertical deformation rates and mountain building in Taiwan from precise leveling and continuous GPS observations, 2000–2008, *J. Geophys. Res.*, *116*, B08406, doi:10.1029/2011JB008242.

Ching, K. E., K. M. Johnson, R. J. Rau, R. Y. Chuang, L. C. Kuo, and P. L. Leu (2011b), Inferred fault geometry and slip distribution of the 2011 Jiashian, Taiwan, earthquake is consistent with a thick-skinned deformation model, *Earth Planet. Sci. Lett.*, *31*, 78–86.

Chuang, R. Y., K. M. Johnson, Y. M. Wu, K. E. Ching, and L. C. Kuo (2013), A midcrustal ramp-fault structure beneath the Taiwan tectonic wedge illuminated by the 2013 Nantou earthquake series, *Geophys. Res. Lett.*, *40*, 5080–5084, doi:10.1002/grl.51005.

Crespi, J. M., Y. C. Chan, and M. S. Swaim (1996), Synorogenic extension and exhumation of the Taiwan hinterland, *Geology*, *24*, 247–250.

Dadson, S. J., et al. (2003), Links between erosion, runoff variability and seismicity in the Taiwan orogen, *Nature*, *426*, 648–651.

Dahlen, F. A., D. Davis, and J. Suppe (1984), Mechanics of fold-and-thrust belts and accretionary wedges: Cohesive Coulomb theory, *J. Geophys. Res.*, *89*, 10,087–10,101, doi:10.1029/JB089iB12p10087.

Davis, D., J. Suppe, and F. A. Dahlen (1983), Mechanics of fold-and-thrust belts and accretionary wedges, *J. Geophys. Res.*, *88*, 1153–1172, doi:10.1029/JB088iB02p01153.

Fisher, D. M., S. Willett, E. En-Chao, and M. B. Clark (2007), Cleavage fronts and fans as reflections of orogen stress and kinematics in Taiwan, *Geology*, *35*, 65–68.

Fuller, C. W., S. D. Willett, D. M. Fisher, and C. Y. Lu (2006), A thermomechanical wedge model of Taiwan constrained by fission-track thermochronology, *Tectonophysics*, *425*, 1–24.

Hsu, Y. J., M. Simons, S. B. Yu, L. C. Kuo, and H. Y. Chen (2003), A two-dimensional dislocation model for interseismic deformation of the Taiwan mountain belt, *Earth Planet. Sci. Lett.*, *211*, 287–294.

Huang, C. Y., P. B. Yuan, and S. J. Tsao (2006), Temporal and spatial records of active arc-continent collision in Taiwan: A synthesis, *GSA Bull.*, *118*, 274–288.

Huang, W. J., K. M. Johnson, J. Fukuda, and S. B. Yu (2010), Insights into active tectonics of eastern Taiwan from analyses of geodetic and geologic data, *J. Geophys. Res.*, *115*, B03413, doi:10.1029/2008JB006208.

Johnson, K. M., P. Segall, and S. B. Yu (2005), A viscoelastic earthquake cycle model for Taiwan, *J. Geophys. Res.*, *110*, B10404, doi:10.1029/2004JB003516.

Kirstein, L. A., M. G. Fellin, S. D. Willett, A. Carter, Y. G. Chen, J. I. Garver, and D. C. Lee (2010), Pliocene onset of rapid exhumation in Taiwan during arc-continent collision: New insights from detrital thermochronometry, *Basin Res.*, *22*, 270–285.

Kuochen, H., Y. M. Wu, C. H. Chang, J. C. Hu, and W. S. Chen (2004), Relocation of eastern Taiwan earthquakes and tectonic implications, *Terr. Atmos. Oceanic Sci.*, *15*, 647–666.

Kuo-Chen, H., F. T. Wu, and S. W. Roecker (2012), Three-dimensional *P* velocity structures of the lithosphere beneath Taiwan from the analysis of TAIGER and related seismic data sets, *J. Geophys. Res.*, *117*, B06306, doi:10.1029/2011JB009108.

Lallemand, S., T. Theunissen, P. Schnürle, C. S. Lee, C. S. Liu, and Y. Font (2013), Indentation of the Philippine Sea plate by the Eurasia plate in Taiwan: Details from recent marine seismological experiments, *Tectonophysics*, *594*, 60–79.

Lee, J. C., J. Angelier, H. T. Chu, J. C. Hu, and F. S. Jeng (2001), Continuous monitoring of an active fault in a plate suture zone: A creepmeter study of the Chihshang Fault, eastern Taiwan, *Tectonophysics*, *333*, 219–240.

Lee, J. C., J. Angelier, H. T. Chu, J. C. Hu, F. S. Jeng, and R. J. Rau (2003), Active fault creep variations at Chihshang, Taiwan, revealed by creep meter monitoring, 1998–2001, *J. Geophys. Res.*, *108*(B11), 2528, doi:10.1029/2003JB002394.

Liu, T. K., S. Hsieh, Y. G. Chen, and W. S. Chen (2001), Thermo-kinematic evolution of the Taiwan oblique-collision mountain belt as revealed by zircon fission track dating, *Earth Planet. Sci. Lett.*, *186*, 45–56.

Malavieille, J., and G. Trullenque (2009), Consequences of continental subduction on forearc basin and accretionary wedge deformation in SE Taiwan: Insights from analogue modeling, *Tectonophysics*, *466*, 377–394.

Malavieille, J., S. E. Lallemand, S. Dominiguez, A. Deschamps, C. Y. Lu, C. S. Liu, P. Schnürle, and the ACT Scientific Crew (2002), Arc-continent collision in Taiwan: New marine observations and tectonic evolution, in *Geology and Geophysics of an Arc-Continent Collision, Taiwan*, *Spec. Pap*., vol. 358, edited by T. B. Byrne and C. S. Liu, pp. 187–211, Geol. Soc. Am, Boulder, Colo.

Mouyen, M., et al. (2009), Expected temporal absolute gravity change across the Taiwanese Orogen, a modeling approach, *J. Geodyn.*, *48*, 284–291.

Mozziconacci, L., B. Delouis, B. S. Huang, J. C. Lee, and N. Béthoux (2013), Determining fault geometry from the distribution of coseismic fault slip related to the 2006 Taitung earthquake, eastern Taiwan, *Bull. Seismol. Soc. Am.*, *103*, 394–411.

Rau, R. J., K. H. Chen, and K. E. Ching (2007), Repeating earthquakes and seismic potential along the northern Longitudinal Valley fault of eastern Taiwan, *Geophys. Res. Lett.*, *34*, L24301, doi:10.1029/2007GL031622.

Rossetti, F., C. Faccenna, and G. Ranalli (2002), The influence of backstop dip and convergence velocity in the growth of viscous doubly-vergent orogenic wedges: Insights from thermomechanical laboratory experiments, *J. Struct. Geol.*, *24*, 953–962.

Shyu, J. B. H., K. Sieh, Y. G. Chen, and C. S. Liu (2005), Neotectonic architecture of Taiwan and its implications for future large earthquakes, *J. Geophys. Res.*, *110*, B08402, doi:10.1029/2004JB003251.

Shyu, J. B. H., K. Sieh, Y. G. Chen, and L. H. Chung (2006), Geomorphic analysis of the Central Range fault, the second major active structure of the Longitudinal Valley suture, eastern Taiwan, *GSA Bull.*, *118*, 1447–1462.

Silver, E. A., and D. L. Reed (1988), Backthrusting in accretionary wedges, *J. Geophys. Res.*, *93*, 3116–3126, doi:10.1029/JB093iB04p03116.

Simoes, M., J. P. Avouac, O. Beyssac, B. Goffé, K. A. Farley, and Y. G. Chen (2007), Mountain building in Taiwan: A thermokinematic model, *J. Geophys. Res.*, *112*, B11405, doi:10.1029/2006JB004824.

Sun, J., K. M. Johnson, Z. Cao, Z. Shen, R. Bürgmann, and X. Xu (2011), Mechanical constraints on inversion of coseismic geodetic data for fault slip and geometry: Example from InSAR observation of the 6 October 2008 *Mw* 6.3 Dangxiong-Yangyi (Tibet) earthquake, *J. Geophys. Res.*, *116*, B01406, doi:10.1029/2010JB007849.

Suppe, J. (1981), Mechanics of mountain building and metamorphism in Taiwan, *Mem. Geol. Soc. China*, *4*, 47–89.

Suppe, J. (2007), Absolute fault and crustal strength from wedge tapers, *Geology*, *35*, 1127–1130.

Teng, L. S., and A. T. Lin (2004), Cenozoic tectonics of the China continental margin: Insights from Taiwan, in *Aspects of the Tectonic Evolution of China*, *Spec. Publ*., vol. 226, edited by J. Malpas et al., pp. 313–332, Geol. Soc., London.

Willemin, J. H., and L. K. Knuepfer (1994), Kinematics of arc-continent collision in the eastern Central Range of Taiwan inferred from geomorphic analysis, *J. Geophys. Res.*, *99*, 20,267–20,280, doi:10.1029/94JB00731.

Willett, S., and M. T. Brandon (2002), On steady states in mountain belts, *Geology*, *30*, 175–178.

Willett, S., C. Beaumont, and P. Fullsack (1993), Mechanical model for the tectonics of doubly vergent compressional orogens, *Geology*, *21*, 371–374.

Willett, S. D., R. Slingerland, and N. Hovius (2001) Uplift, shortening, and steady state topography in active mountain belts, *Am. J. Sci.*, *301*, 455–485.

Willett, S., D. Fisher, C. Fuller, E. C. Yeh, and C. Y. Lu (2003), Erosion rates and orogenic-wedge kinematics in Taiwan inferred from fission-track thermochronometry, *Geology*, *31*, 945–948.

Wu, Y. M., and C. F. Wu (2007), Approximate recovery of coseismic deformation from Taiwan strong-motion records, *J. Seismol.*, *11*, 159–170.

Wu, Y. M., Y. G. Chen, C. H. Chang, L. H. Chung, T. L. Teng, F. T. Wu, and C. F. Wu (2006) Seismogenic structure in a tectonic suture zone: With new constraints from 2006 Mw6.1 Taitung earthquake, *Geophys. Res. Lett.*, *33*, L22305, doi:10.1029/2006GL027572.

Wu, Y. M., C. H. Chang, L. Zhao, T. L. Teng, and M. Nakamura (2008), A comprehensive relocation of earthquakes in Taiwan from 1991 to 2005, *Bull. Seismol. Soc. Am.*, *98*, 1471–1481.

Wu, Y. M., J. B. H. Shyu, C. H. Chang, L. Zhao, M. Nakamura, and S. K. Hsu (2009), Improved seismic tomography offshore northeastern Taiwan: Implications for subduction and collision processes between Taiwan and the southernmost Ryukyu, *Geophys. J. Int.*, *178*, 1042–1054.

Yen, T. P. (1965), A thrust fault near Juisui, eastern Taiwan, *Proc. Geol. Soc. China*, *8*, 97–99.

Yu, S. B., H. Y. Chen, and L. C. Kuo (1997), Velocity field of GPS stations in the Taiwan area, *Tectonophysics*, *274*, 41–59.

Yue, L. F., J. Suppe, and J. J. Hung (2005), Structural geology of a classic thrust belt earthquake: The 1999 Chi-Chi earthquake Taiwan (Mw = 7.6), *J. Struct. Geol.*, *27*, 2058–2083.

